

Mollow triplet: pump probe single photon spectroscopy of artificial atoms

A. N. Sultanov¹ and Ya. S. Greenberg^{1,*}

¹*Novosibirsk State Technical University, Novosibirsk, Russia*

(Dated: January 27, 2023)

We analyze a photon transport through an open waveguide side coupled to the microwave cavity with imbedded artificial atom (qubit). Qubit is driven by a strong signal with the frequency close to the resonators first harmonic. The qubit state is probed by a weak signal at the fundamental frequency of the waveguide. Within the formalism of projection operators and non-Hermitian Hamiltonian approach we develop a one-photon approximation scheme for the calculation of the transmission and reflection factors of the microwave signal through a waveguide. We obtain analytic expressions for the transmission and reflection amplitudes of the Mollow triplet, which contain the information of the qubit parameters. We show that for small number of cavity photons the transmission and reflection spectra consist of four peaks that is a direct manifestation of quantum nature of light.

The results obtained in the paper are of general nature and can be applied to any type of qubits. The specific properties of the qubit are only encoded in the two parameters: the energy Ω of the qubit and its coupling λ to the cavity photons.

PACS numbers: 84.40.Az, 84.40.Dc, 85.25.Hv, 42.50.Dv, 42.50.Pq

I. INTRODUCTION

The coherent coupling of a superconducting qubit to the microwave modes of a 1D coplanar waveguide transmission line has been intensely investigated over the last years both experimentally and theoretically. Compared with the conventional optical cavity with atomic gases, superconducting qubits as artificial atoms in solid-state devices have significant advantages, such as technological scalability, long coherence time which is important for the implementation of the quantum gate operations, huge tunability and controllability by external electromagnetic fields¹⁻⁴. Another advantage is an on-chip realization of ultrastrong coupling regime⁵ previously inaccessible to atomic systems that enables us to explore novel quantum phenomena emerging only in this regime. Furthermore, solid state superconducting circuits with embedded Josephson junction qubits have reproduced many physical phenomena known previously from quantum optics, such as Kerr nonlinearities⁶, electromagnetically induced transparency⁷⁻⁹, the Mollow triplet¹⁰⁻¹⁴, and Autler-Townes doublet^{10,15}.

As the Mollow triplet is a clear manifestation of the coherent nature of the light- matter interaction, its fluorescent or transmission spectra can be explained considering the pumping light classically¹⁶. The use of a single photon source as a pump or squeezed vacuum reveals a marked influence of the quantum nature of light on the Mollow spectra^{13,14}.

In the present paper we consider the transmission and reflection Mollow spectra for artificial atom (qubit) embedded in the N - photon cavity which is side- coupled to microwave transmission line.

Our analysis is based on the projection operators formalism and the method of the effective non- Hermitian Hamiltonian which has many applications for different open mesoscopic systems (see review paper¹⁷ and references therein). Recently this method has been applied to electron and photon transport through 1D solid state nanostructures¹⁸⁻²⁰.

We show that for small number of cavity photons the transmission and reflection spectra consist of four peaks which is a direct manifestation of quantum nature of light. As the num-

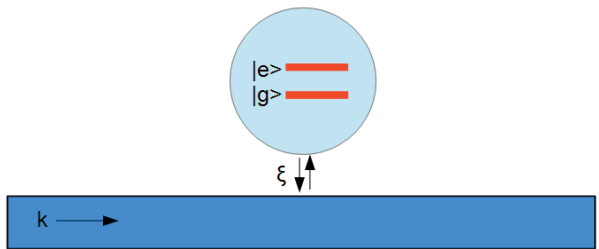


FIG. 1: Waveguide side coupled to the N - photon cavity with imbedded qubit

ber of cavity photons is increased two central peaks merge giving classical Mollow triplet.

The paper is organized as follows. In Sec. II we write down the Hamiltonian of 1D waveguide side coupled to the N - photon microwave cavity with imbedded qubit. In Sec. III the projection operators formalism and the method of effective non hermitian Hamiltonian are briefly reviewed. This method is applied to one photon scattering in Sec.IV. We give analytical expression for the effective non hermitian Hamiltonian and find the spectrum of the cavity resonances and the dependence of their widths on the cavity decay rate Γ . The wave function of the Mollow triplet is found in Sec.V. We obtain the explicit analytical expressions for the transmission and reflection amplitudes and show representative photon spectra.

II. THE MODEL HAMILTONIAN

We consider a microwave 1D waveguide side coupled to a resonator with imbedded qubit as is shown in Fig.1.

The Hamiltonian of the system reads:

$$H = H_{ph} + H_{qb} + H_c + H_{c-qb} + H_{w-c} \quad (1)$$

where H_{ph} is the Hamiltonian of waveguide photons, H_{qb} is the Hamiltonian of the qubit with the excitation frequency Ω ,

H_c is the Hamiltonian of one mode resonator, H_{cqb} is the qubit-resonator interaction, and H_{w-c} is the interaction between the waveguide and the resonator.

$$H_{ph} = \sum_k \hbar \omega_k c_k^+ c_k \quad (2)$$

$$H_{qb} = \frac{1}{2} \hbar \Omega \sigma_z \quad (3)$$

$$H_r = \hbar \omega_c a^+ a \quad (4)$$

$$H_{\text{int}}^{q-r} = \hbar \lambda (a^+ + a) \sigma_X \quad (5)$$

$$H_{\text{int}}^{wg-r} = \hbar \xi \sum_k (c_k^+ a + c_k a^+) \quad (6)$$

III. PROJECTION FORMALISM AND EFFECTIVE NON-HERMITIAN HAMILTONIAN

Here we briefly describe the essence of this method omitting its rigorous justification which can be found in the corresponding literature¹⁷. The application of this method to photon transport was described in more detail in²⁰.

According to this method the Hilbert space of a quantum system with the Hermitian Hamiltonian H is formally subdivided into two arbitrarily selected orthogonal projectors, P and Q , which satisfy the following properties:

$$P + Q = 1; \quad PQ = QP = 0; \quad PP = P; \quad QQ = Q \quad (7)$$

The solution of the stationary Schrödinger equation,

$$H\Psi = E\Psi \quad (8)$$

in general consists of two parts,

$$\Psi \equiv P\Psi + Q\Psi \equiv \Psi_P + \Psi_Q \quad (9)$$

Hamiltonian (8) acts within each subspace. If we eliminate the P -subspace, the equation for the wave function in Q -subspace takes the form

$$H_{\text{eff}}(E)\Psi_Q = E\Psi_Q \quad (10)$$

where the *energy dependent* effective Hamiltonian

$$H_{\text{eff}}(E) = H_{QQ} + H_{QP} \frac{1}{E - H_{PP}} H_{PQ} \quad (11)$$

projects Hilbert space on the Q subspace. In Eq.11 $H_{XY} = XHY$, where X, Y stands for Q or P . It is also worth to note that $PH_{\text{eff}} = H_{\text{eff}}P = 0$.

Keeping in mind the scattering problem we assume that Q subspace consists of discrete states, and P subspace consists of the states from continuum. In order to avoid the singularities emerging when H_{PP} has eigenvalues at real energy E , it has to be considered as a limiting value from the upper half of the complex energy plane, $E^+ = E + i\varepsilon$. With this rule, those states of subspace Q which will turn out to be coupled to the states in subspace P will acquire the outgoing waves and become unstable. Then, for this scattering problem the effective Hamiltonian (11) becomes non Hermitian and has to be written as follows:

$$H_{\text{eff}}(E) = H_{QQ} + H_{QP} \frac{1}{E - H_{PP} + i\varepsilon} H_{PQ} \quad (12)$$

In this case the equation (10) defines the resonance energies of the Q -system which lie in the low half of the complex energy plane, $E = \tilde{E} - i\hbar\tilde{\Gamma}$ and are given by the roots of the equation

$$D(E) \equiv \det(E - H_{\text{eff}}) = 0 \quad (13)$$

The imaginary part $\tilde{\Gamma}$ of the resonances describes the decay of Q -states due to their interaction with P -states.

The scattering solution for the state vector of the Shrödinger wavefunction Ψ reads²¹

$$|\Psi\rangle = |in\rangle + \frac{1}{E - H_{\text{eff}}} H_{QP} |in\rangle + \frac{1}{E - H_{PP} + i\varepsilon} \frac{1}{E - H_{\text{eff}}} H_{PQ} |in\rangle \quad (14)$$

where $|in\rangle$ is the initial state, which contains continuum variables and satisfies the equation $H_{PP}|in\rangle = E|in\rangle$, where E is the same as in (8).

In fact, the expression (14) is nothing more than a decomposition (9) where the last term is the part of Ψ_P , which describes to all orders of H_{QP} the evolution of initial state $|in\rangle$ under the interaction between P and Q subspaces.

IV. THE SCATTERING IN THE ONE PHOTON APPROXIMATION

We consider below one photon approximation when there are one or none photons in the waveguide. We also populate the resonator with N cavity photons, so that our Hilbert space is restricted to the following state vectors:

$$|1\rangle \equiv |0, N, g\rangle, \quad |2\rangle \equiv |0, N-1, e\rangle \quad (15)$$

$$|k_1\rangle \equiv |k, N-1, g\rangle, \quad |k_2\rangle \equiv |k, N-2, e\rangle \quad (16)$$

In Eq.15 the state $|1\rangle$ corresponds to no photons in a waveguide, N photons in the cavity, and a qubit in a ground state g . The state $|2\rangle$ corresponds to no photons in a waveguide, $N-1$ photons in the cavity, and a qubit in an excited state e .

The states in Eq.16 correspond to the situation where one photon leave the cavity (states (15)) into a waveguide. The state $|k_1\rangle$ corresponds to one photon with a momentum k in a waveguide, $N - 1$ photons in the cavity, and a qubit in a ground state g . The state $|k_2\rangle$ corresponds to one photon in a waveguide, $N - 2$ photons in the cavity, and a qubit in an excited state e .

In accordance with the projection operators formalism we define two mutual orthogonal subspaces as follows

$$Q = |1\rangle\langle 1| + |2\rangle\langle 2| \quad (17)$$

$$P = \sum_k \sum_{n=1}^2 |k_n\rangle\langle k_n| = \frac{L}{2\pi} \int dk \sum_{n=1}^2 |k_n\rangle\langle k_n| \quad (18)$$

where L is the length of waveguide, and the orthogonality condition for P subspace vectors is

$$\langle k_n | k'_m \rangle = \frac{2\pi}{L} \delta_{n,m} \delta(k_n - k'_m) \quad (19)$$

where $n, m = 1, 2$.

The application of the method requires the continuum state vectors to be the eigenfunctions of Hamiltonian H_{PP} . This is not the case for (16) since H_{PP} couples two vectors $|k_1\rangle$ and $|k_2\rangle$. Therefore, first it is necessary to find the eigenfunctions of H_{PP} within the subspace of state vectors (16).

$$|\varphi_{i,k}\rangle = a_i |k_1\rangle + b_i |k_2\rangle = |k\rangle \otimes |\varphi_i\rangle \quad (20)$$

where

$$|\varphi_i\rangle = a_i |N-1, g\rangle + b_i |N-2, e\rangle \quad (21)$$

State vectors $|\varphi_{i,k}\rangle$, $i = 1, 2$ are eigenfunctions of H_{PP} with the energies

$$E_i/\hbar = -\frac{1}{2}\omega_c + \omega_c(N-1) + \omega_k - \frac{1}{2}(-1)^i \Omega_R \quad (22)$$

with Rabi frequency

$$\Omega_R = \sqrt{(\omega_c - \Omega)^2 + 4\lambda^2(N-1)} \quad (23)$$

The superposition factors a_i and b_i are as follows:

$$a_1 = \frac{1}{\sqrt{2}} \sqrt{1 - \frac{\Omega - \omega_c}{\Omega_R}} \quad b_1 = \frac{1}{\sqrt{2}} \sqrt{1 + \frac{\Omega - \omega_c}{\Omega_R}} \quad (24)$$

$$a_2 = -\frac{1}{\sqrt{2}} \sqrt{1 + \frac{\Omega - \omega_c}{\Omega_R}} \quad b_2 = \frac{1}{\sqrt{2}} \sqrt{1 - \frac{\Omega - \omega_c}{\Omega_R}} \quad (25)$$

The matrix of H_{eff} in the Q subspace is as follows

$$\begin{aligned} \langle m | H_{eff} | n \rangle &= \langle m | H_{QQ} | n \rangle \\ &- i \frac{L}{v_g} \sum_{i=1}^2 \langle m | H_{QP} | \varphi_{i,k} \rangle \langle \varphi_{i,k} | H_{PQ} | n \rangle \end{aligned} \quad (26)$$

With the aid of (20) we obtain the elements of the matrix (26)

$$\langle 1 | H_{eff} | 1 \rangle = \omega_c N - \frac{1}{2}\Omega - jN\Gamma \quad (27a)$$

$$\langle 2 | H_{eff} | 2 \rangle = \omega_c(N-1) + \frac{1}{2}\Omega - j(N-1)\Gamma \quad (27b)$$

$$\langle 1 | H_{eff} | 2 \rangle = \langle 2 | H_{eff} | 1 \rangle = \lambda\sqrt{N} \quad (27c)$$

where we introduce the width of the cavity decay rate $\Gamma = L\xi^2/v_g$. The details of the calculation of Eqs. 26, 27a, 27b, 27c are given in the Appendix.

A. Resonances in the Q subsystem

Due to the interaction of the Q states (15) with continuum states (16) the former acquire the resonances whose energies and widths become dependent on the coupling parameter ξ in Hamiltonian (6), which defines the width of the cavity decay rate Γ . These resonances are given by the complex roots of Eq.13. For H_{eff} given by the matrix elements 27a, 27b, 27c this equation reads:

$$\begin{aligned} D(E) &= \left(E/\hbar + \frac{1}{2}\Omega - \omega_c N + jN\Gamma \right) \\ &\times \left(E/\hbar - \frac{1}{2}\Omega - \omega_c(N-1) + j(N-1)\Gamma \right) - \lambda^2 N = 0 \end{aligned} \quad (28)$$

Every of two Q states (15) may decay in two ways: either to the state $|\varphi_{1,k}\rangle$ with the energy

$$E_1/\hbar = \omega + \omega_c N - \frac{3}{2}\omega_c + \frac{\Omega_R}{2} \quad (29)$$

or to the state $|\varphi_{2,k}\rangle$ with the energy

$$E_2/\hbar = \omega + \omega_c N - \frac{3}{2}\omega_c - \frac{\Omega_R}{2} \quad (30)$$

where ω is the frequency of incident photon.

Accordingly, for the roots in both cases we obtain:

$$\begin{aligned} D(E_1) &= \left(\delta - \frac{\Delta}{2} + \frac{\Omega_R}{2} + jN\Gamma \right) \\ &\times \left(\delta + \frac{\Delta}{2} + \frac{\Omega_R}{2} + j(N-1)\Gamma \right) - \lambda^2 N = 0 \end{aligned} \quad (31a)$$

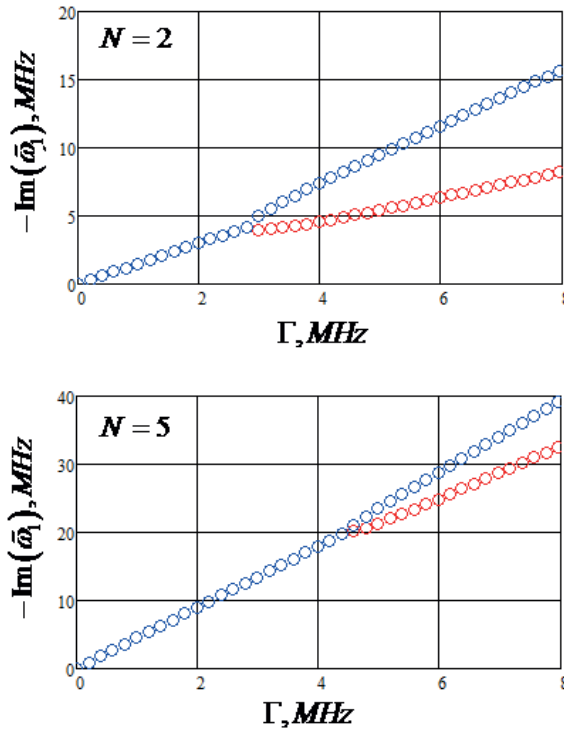


FIG. 2: The dependence of the resonance widths on the cavity decay rate Γ for $\Delta = 0$.

$$D(E_2) = \left(\delta - \frac{\Delta}{2} - \frac{\Omega_R}{2} + jN\Gamma \right) \times \left(\delta + \frac{\Delta}{2} - \frac{\Omega_R}{2} + j(N-1)\Gamma \right) - \lambda^2 N = 0 \quad (31b)$$

where we introduced detunings $\delta = \omega - \omega_c$, $\Delta = \omega_c - \Omega$.

The solutions of these equations for the resonances in frequency domain ($\tilde{\omega} = E/\hbar$) are:

$$\tilde{\omega}_{1,\pm} = \omega_C - \frac{1}{2} [\Omega_R + j(2N-1)\Gamma] \pm \frac{1}{2} \sqrt{(\Delta - j\Gamma)^2 + 4\lambda^2 N} \quad (32a)$$

$$\tilde{\omega}_{2,\pm} = \omega_C + \frac{1}{2} [\Omega_R - j(2N-1)\Gamma] \pm \frac{1}{2} \sqrt{(\Delta - j\Gamma)^2 + 4\lambda^2 N} \quad (32b)$$

Since $\tilde{\omega}_{2,\pm} = \tilde{\omega}_{1,\pm} + \Omega_R$, the dependence of these resonances on Γ is the same for both cases. The dependence of the width on Γ is shown in Fig.2 for $\Delta = 0$. The position of splitting corresponds to the point $2\lambda\sqrt{N} = \Gamma$.

The dependence of resonance energies on Γ for $\Delta = 0$ is shown in Fig.3. For $\Gamma > 2\lambda\sqrt{N}$ the resonance energies do not depend on Γ . For nonzero detuning Δ The energies are split for any Γ as shown in Fig.4. As the detuning is increased the real part of $\tilde{\omega}_{1,+}$ tends to ω_c , while the real part of $\tilde{\omega}_{1,-}$ scales as $\omega_c - \Delta$.

Below we show the frequency spectra of $1/|D(E_1)|$ and $1/|D(E_2)|$ for zero detuning $\Delta = 0$ and for intermediate $\lambda \sim$

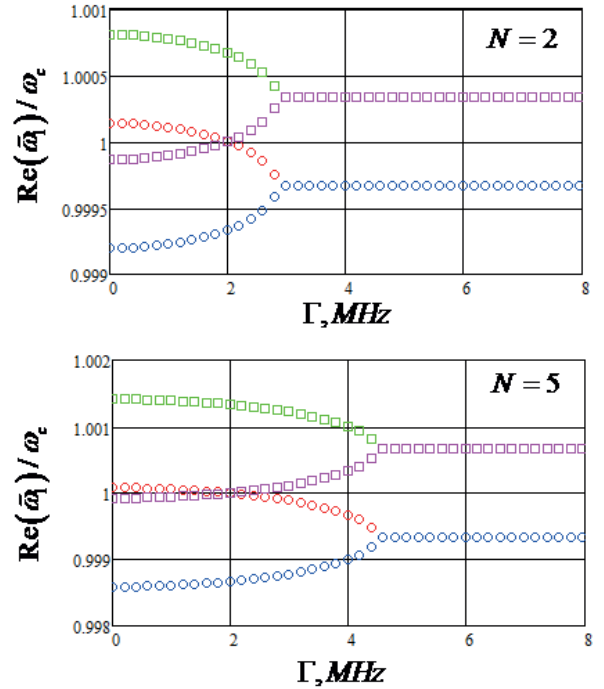


FIG. 3: The dependence of resonance energy on Γ for $\Delta = 0$. Upper curve corresponds to $\tilde{\omega}_{2,\pm}$, the lower one- to $\tilde{\omega}_{1,\pm}$.

Γ (Fig.5) and strong $\lambda \gg \Gamma$ (Fig.6) coupling. As can be seen from Fig.6 the resonances are well resolved for the case of strong coupling.

We will see below that the peaks of these resonances and their widths coincide with those of Mollow triplet. The dependence of the resonance peaks on the coupling strength between qubit and cavity photons is shown in Fig.7 for zero detuning and $N = 5$.

V. THE WAVE FUNCTION OF THE MOLLOW TRIPLET

The key notion for the subsequent calculation of photon transmission and reflection is a transmission matrix

$$\begin{aligned} & \langle j, k' | T | k, i \rangle \\ &= \sum_{n,m=1}^2 \langle \varphi_{j,k'} | H_{PQ} | n \rangle R_{n,m}(E_i) \langle m | H_{QP} | \varphi_{i,k} \rangle \end{aligned} \quad (33)$$

where $R_{m,n}(E)$ is the matrix inverse of the matrix $\langle m | (E - H_{eff}) | n \rangle$:

$$R_{n,m}(E) = \langle n | \frac{1}{E - H_{eff}} | m \rangle \quad (34)$$

From (27a), (27b), (27c) we find the elements of R matrix

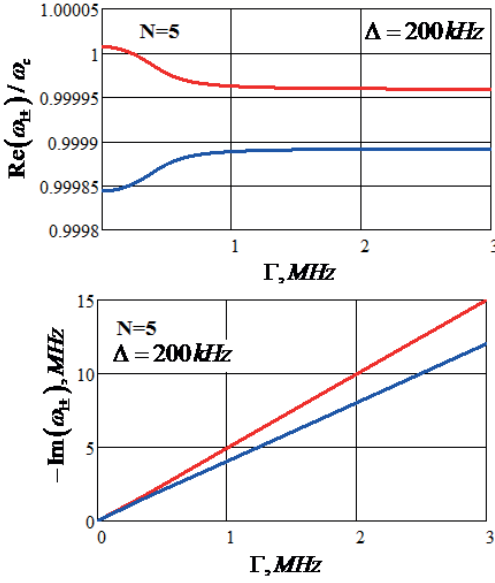


FIG. 4: The dependence of real (upper plot) and imaginary (lower plot) parts of $\tilde{\omega}_{1,\pm}$ on Γ for nonzero detuning. The red curve corresponds to $\tilde{\omega}_{1,+}$, while the blue curve corresponds to $\tilde{\omega}_{1,-}$

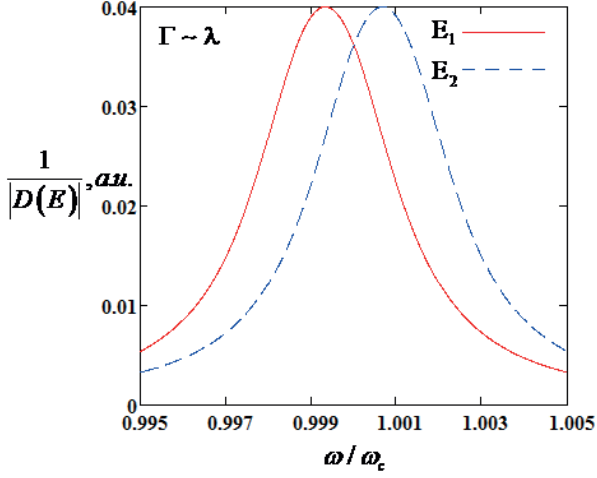


FIG. 5: The frequency spectra of $1/|D(E_1)|$ and $1/|D(E_2)|$ for zero detuning $\Delta = 0$ and for intermediate $\lambda \sim \Gamma$ coupling.

(34).

$$R_{11}(E) = \frac{1}{D(E)} \left(E - \omega_C(N-1) - \frac{1}{2}\Omega + j(N-1)\Gamma \right) \quad (35a)$$

$$R_{22}(E) = \frac{1}{D(E)} \left(E - \omega_C N + \frac{1}{2}\Omega + jN\Gamma \right) \quad (35b)$$

$$R_{12}(E) = R_{21}(E) = \frac{\lambda\sqrt{N}}{D(E)} \quad (35c)$$

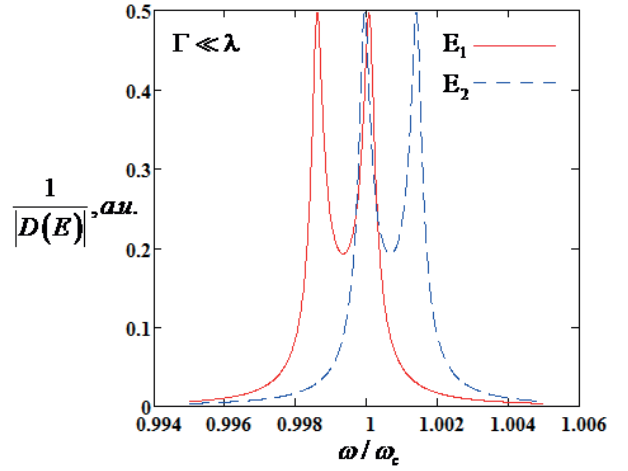


FIG. 6: The frequency spectra of $1/|D(E_1)|$ and $1/|D(E_2)|$ for zero detuning $\Delta = 0$ and for strong $\lambda \gg \Gamma$ coupling.

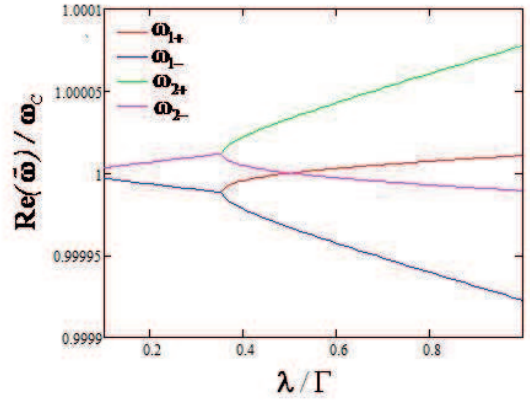


FIG. 7: The dependence of the resonance peaks on the coupling strength between qubit and cavity photons for $\Delta = 0$ and $N = 5$.

where $D(E)$ is given in (28).

In our case the transmission matrix (33) does not depend on the final momentum k' (detail are given in Appendix). The dependence of (33) on initial momentum k is hidden in the energies E_i (29), (30) which depend on the frequency ω of incident photon. Therefore, below we use the concise form of the transmission matrix: $\langle j, k' | T | i, k \rangle = \langle \varphi_j | T | \varphi_i \rangle \equiv \xi^2 t_{j,i}$. The calculations, the details of which are given in the Appendix, yield the following expressions for the elements of transmission matrix.

$$t_{11} = \frac{1}{4\Omega_R D(E_1)} [N(\Omega_R + \Delta)(2\delta + \Delta + \Omega_R) + (N-1)(\Omega_R - \Delta)(2\delta - \Delta + \Omega_R) + 4jN(N-1)\Omega_R\Gamma + 8\lambda^2 N(N-1)] \quad (36)$$

$$t_{21} = -\frac{\lambda\sqrt{N-1}}{2\Omega_R D(E_1)} (2\delta + \Omega_R - \Delta) \quad (37)$$

$$t_{22} = \frac{1}{4\Omega_R D(E_2)} [N(\Omega_R - \Delta)(2\delta + \Delta - \Omega_R) + (N-1)(\Omega_R + \Delta)(2\delta - \Omega_R - \Delta) + 4jN(N-1)\Omega_R\Gamma - 8\lambda^2 N(N-1)] \quad (38)$$

$$t_{21} = -\frac{\lambda\sqrt{N-1}}{2\Omega_R D(E_2)} (2\delta - \Omega_R - \Delta) \quad (39)$$

The quantity (33) describes the process where the incident photon with momentum k comes into interaction with a cavity that was initially in the state $|\varphi_i\rangle$ and then leaves with momentum k' leaving the cavity in the state $|\varphi_j\rangle$. Therefore, four different outcomes of this scattering processes for transmitted probe signal are possible: two of them correspond to elastic scattering and two of them correspond to inelastic process with the momenta of outgoing photon $k' = k \pm \Omega_R/v_g$ (see Fig.8). According to these possibilities the initial state $|in\rangle$ in (14) corresponds to either $|\varphi_{1,k}\rangle$ or $|\varphi_{2,k}\rangle$.

$$|\Psi_1\rangle = |\varphi_{1,k}\rangle + \sum_{m,n} |n\rangle R_{nm}(E_1) \langle m| H_{QP} |\varphi_{1,k}\rangle + \sum_{q,i} \frac{|\varphi_{i,q}\rangle}{E_1(k) - E_i(q) + i\varepsilon} \langle i, q| T |1, k\rangle \quad (40)$$

$$|\Psi_2\rangle = |\varphi_{2,k}\rangle + \sum_{m,n} |n\rangle R_{nm}(E_2) \langle m| H_{QP} |\varphi_{2,k}\rangle + \sum_{q,i} \frac{|\varphi_{i,q}\rangle}{E_2(k) - E_i(q) + i\varepsilon} \langle i, q| T |2, k\rangle \quad (41)$$

From (40), (41) we obtain the photon wavefunctions in the configuration space $\langle x|\Psi_1\rangle$ and $\langle x|\Psi_2\rangle$:

$$\langle x|\Psi_1\rangle = e^{ikx} |\varphi_1\rangle - i\Gamma e^{ik|x|} t_{11} |\varphi_1\rangle - i\Gamma e^{i(k + \frac{\Omega_R}{v_g})|x|} t_{12} |\varphi_2\rangle \quad (42)$$

$$\langle x|\Psi_2\rangle = e^{ikx} |\varphi_2\rangle - i\Gamma e^{ik|x|} t_{22} |\varphi_2\rangle - i\Gamma e^{i(k - \frac{\Omega_R}{v_g})|x|} t_{21} |\varphi_1\rangle \quad (43)$$

The equations (42) and (43) are the main results of our paper. They have a clear physical sense. The transmission signal (at $x > 0$) consists of four waves: two elastic scattering waves with transmission factors $T_{11} = 1 - i\Gamma t_{11}$, $T_{22} = 1 - i\Gamma t_{22}$, and two inelastic scattering waves with transmission factors $T_{12} = -i\Gamma t_{12}$, $T_{21} = -i\Gamma t_{21}$.

Below we define the overall transmission factor for small number of cavity photons. In this case we must take into account the effect of photon blockade¹³: a probing scattering

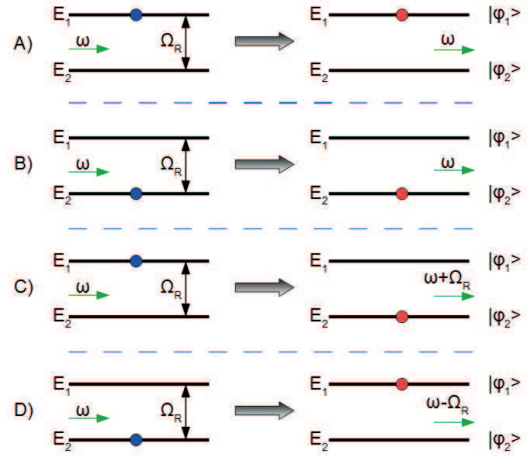


FIG. 8: Four outcomes of the scattering process. Two upper graphs correspond to elastic scattering, while two lower graphs correspond to inelastic sidebands. Blue circles denote the initial state, red ones denote the final state.

photon can enter the cavity only after a preceding photon left it. For every photon there are two ways of the scattering depending on the initial state the system was before the scattering (see Fig.8). This is seen in Eqs. (42) and (43) where the every scattering route is a superposition of two final states $|\varphi_1\rangle$ and $|\varphi_2\rangle$. Since for single photon probe the scattering processes for two initial states are independent, we define the overall transmission for $x > 0$ as:

$$|T|^2 \equiv |\langle x|\Psi_1\rangle|^2 + |\langle x|\Psi_2\rangle|^2 = 2 + \Gamma^2 |t_{11}|^2 + \Gamma^2 |t_{12}|^2 + i\Gamma (t_{11}^* - t_{11}) + \Gamma^2 |t_{22}|^2 + \Gamma^2 |t_{21}|^2 + i\Gamma (t_{22}^* - t_{22}) \quad (44)$$

Accordingly, the reflection is defined for $x < 0$ as:

$$|R|^2 \equiv |\langle x|\Psi_1\rangle - e^{ikx} |\varphi_1\rangle|^2 + |\langle x|\Psi_2\rangle - e^{ikx} |\varphi_2\rangle|^2 = \Gamma^2 |t_{11}|^2 + \Gamma^2 |t_{12}|^2 + \Gamma^2 |t_{22}|^2 + \Gamma^2 |t_{21}|^2 \quad (45)$$

Below we show the transmission coefficients as function of the frequency of incident photon for the case of intermediate (Fig.9) and strong (Fig.10) coupling.

The full reflection spectrum (45) is shown on Fig.11. The four spectral peaks in this figure is a direct manifestation of the quantum nature of light: for small number of cavity photons N the distance between the Rabi levels in neighbor manifolds is not equal to each other: $\Omega_R^{(N)} > \Omega_R^{(N-1)}$. These Rabi frequencies can be readily found from Fig.11: a distance between main peaks is $\frac{1}{2}(\Omega_R^{(N)} - \Omega_R^{(N-1)})$, and a distance between sidebands is $\frac{1}{2}(\Omega_R^{(N)} + \Omega_R^{(N-1)})$.

VI. CONCLUSION

We develop a theoretical method for the calculation of a photon transport in a waveguide side coupled to a resonant

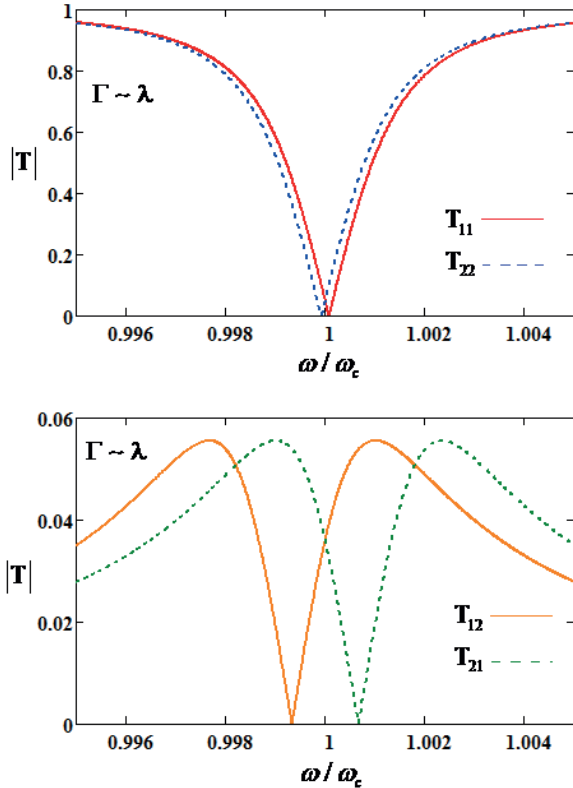


FIG. 9: Transmission factors vs frequency for zero detuning $\Delta = 0$ and intermediate coupling.

microwave cavity with imbedded artificial atom (qubit). We show that if the number of the cavity photons is small the transmitted and reflected spectra reveal a quadruplet structure with two central peaks and two sidebands. This is the direct manifestation of the quantum nature of light which results in a different space between Rabi levels in adjacent manifolds. As the number of the cavity photons is increased the two central peaks merge giving a classical Mollow triplet.

ACKNOWLEDGMENTS

We acknowledge the financial support from the Russian Science Foundation under grant No.16-19-10069

Appendix A: The calculation of H_{XY}

With the aid of explicit expressions (17) and (18) for Q and P we obtain for the parts H_{XY} of the full Hamiltonian (1) the following expressions:

$$H_{QQ} = \frac{1}{2}\hbar\Omega|2\rangle\langle 2| - \frac{1}{2}\hbar\Omega|1\rangle\langle 1| + \hbar\omega_c(N-1)|2\rangle\langle 2| + \hbar\lambda\sqrt{N}|1\rangle\langle 2| + \hbar\lambda\sqrt{N}|2\rangle\langle 1| + \hbar\omega_cN|1\rangle\langle 1| \quad (\text{A1})$$

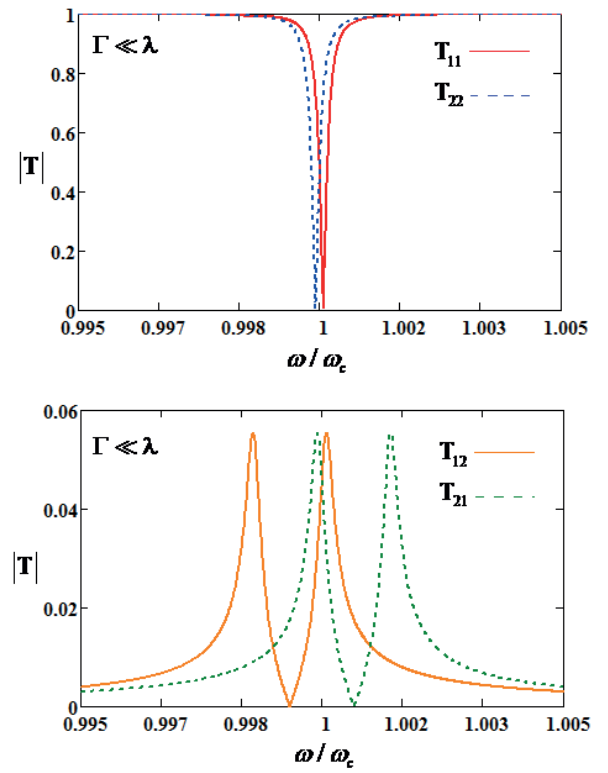


FIG. 10: Transmission factors vs frequency for zero detuning $\Delta = 0$ and strong coupling

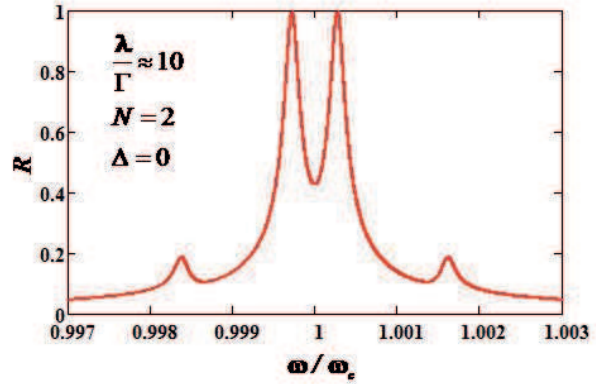


FIG. 11: Overall reflection spectrum as given by the expression (45)

$$\begin{aligned}
H_{PP} &= \frac{1}{2}\hbar\Omega \sum_k |k_2\rangle\langle k_2| + \hbar\omega_c (N-1) \sum_k |k_1\rangle\langle k_1| \\
&+ \hbar\lambda\sqrt{N-1} \sum_k |k_1\rangle\langle k_2| + \hbar\lambda\sqrt{N-1} \sum_k |k_2\rangle\langle k_1| \\
&+ \sum_k \hbar\omega_k |k_1\rangle\langle k_1| + \sum_k \hbar\omega_k |k_2\rangle\langle k_2| \\
&+ \hbar\omega_c (N-2) \sum_k |k_2\rangle\langle k_2| - \frac{1}{2}\hbar\Omega \sum_k |k_1\rangle\langle k_1| \quad (\text{A2})
\end{aligned}$$

$$H_{PQ} = \hbar\xi\sqrt{N-1} \sum_k |k_2\rangle\langle 2| + \hbar\xi\sqrt{N} \sum_k |k_1\rangle\langle 1| \quad (\text{A3})$$

$$H_{QP} = \hbar\xi\sqrt{N} \sum_k |1\rangle\langle k_1| + \hbar\xi\sqrt{N-1} \sum_k |2\rangle\langle k_2| \quad (\text{A4})$$

Appendix B: Calculation of the effective Hamiltonian

From (11) we find the matrix elements of effective hamiltonian in Q subspace.

$$\begin{aligned}
\langle m | H_{eff} | n \rangle &= \langle m | H_{QQ} | n \rangle \\
&+ \sum_{\substack{i,j=1 \\ k,k'}}^2 \langle m | H_{QP} | \varphi_{i,k} \rangle \langle \varphi_{i,k} | \frac{1}{E - H_{PP} + i\varepsilon} | \varphi_{j,k'} \rangle \langle \varphi_{j,k'} | H_{PQ} | n \rangle \\
&= \langle m | H_{QQ} | n \rangle + \sum_{i=1, k}^{i=2} \frac{\langle m | H_{QP} | \varphi_{i,k} \rangle \langle \varphi_{i,k} | H_{PQ} | n \rangle}{E - E_i(k) + i\varepsilon} \quad (\text{B1})
\end{aligned}$$

Fortunately, the matrix elements $\langle m | H_{QP} | \varphi_{i,k} \rangle$ and $\langle \varphi_{i,k} | H_{PQ} | n \rangle$ do not depend on the photon momentum k . The direct calculations yield:

$$\langle 1 | H_{QP} | \varphi_{1,k} \rangle = a_1 \xi \sqrt{N}, \quad \langle 2 | H_{QP} | \varphi_{1,k} \rangle = b_1 \xi \sqrt{N-1} \quad (\text{B2})$$

$$\langle 1 | H_{QP} | \varphi_{2,k} \rangle = a_2 \xi \sqrt{N}, \quad \langle 2 | H_{QP} | \varphi_{2,k} \rangle = b_2 \xi \sqrt{N-1} \quad (\text{B3})$$

With the use of (A1) and (B2), (B3) we obtain for the matrix elements of (B1):

$$\langle 1 | H_{eff} | 1 \rangle = \omega_C N - \frac{1}{2}\Omega + a_1^2 \xi^2 N J_1(E) + a_2^2 \xi^2 N J_2(E) \quad (\text{B4a})$$

$$\begin{aligned}
\langle 2 | H_{eff} | 2 \rangle &= \omega_C (N-1) + \frac{1}{2}\Omega + b_1^2 \xi^2 (N-1) J_1(E) \\
&+ b_2^2 \xi^2 (N-1) J_2(E) \quad (\text{B4b})
\end{aligned}$$

$$\begin{aligned}
\langle 1 | H_{eff} | 2 \rangle &= \langle 2 | H_{eff} | 1 \rangle = \lambda \sqrt{N} \\
&+ a_1 b_1 \xi^2 \sqrt{N(N-1)} J_1(E) + a_2 b_2 \xi^2 \sqrt{N(N-1)} J_2(E) \quad (\text{B4c})
\end{aligned}$$

where

$$J_j(E) = \sum_k \frac{1}{E - E_j(k) + i\varepsilon} = \frac{L}{2\pi} \int \frac{dk}{E - E_j(k) + i\varepsilon} \quad (\text{B5})$$

It will be shown below that all quantities $J_j(E)$ in (B4a), (B4b), and (B4c) are the same and do not depend on the running energy E .

$$J_j(E) = -\frac{2\pi i}{v_g} \quad (\text{B6})$$

where v_g is the velocity of microwave photons in a waveguide.

Finally, with the use of properties of coefficients (24), (25) $a_1^2 + a_2^2 = 1$, $b_1^2 + b_2^2 = 1$, $a_1 b_1 + a_2 b_2 = 0$ we obtain for the matrix elements of H_{eff} the expressions (27a), (27b), (27c) which are given in the main text.

Appendix C: Calculation of transmission matrix (33)

As was shown in Sec.V, $\langle j, k' | T | i, k \rangle = \langle \varphi_j | T | \varphi_i \rangle \equiv \xi^2 t_{j,i}$. With the aid of (B2), (B3) we obtain for matrix t_{ij} the following expressions:

$$\begin{aligned}
t_{11} &= (a_1^2 N R_{11}(E_1) + b_1^2 (N-1) R_{22}(E_1) \\
&+ 2a_1 b_1 \sqrt{N(N-1)} R_{12}(E_1)) \quad (\text{C1a})
\end{aligned}$$

$$\begin{aligned}
t_{12} &= (a_1 a_2 N R_{11}(E_1) + b_1 b_2 (N-1) R_{22}(E_1) \\
&+ \sqrt{N(N-1)} (a_2 b_1 + a_1 b_2) R_{12}(E_1)) \quad (\text{C1b})
\end{aligned}$$

$$\begin{aligned}
t_{22} &= (a_2^2 N R_{11}(E_2) + b_2^2 (N-1) R_{22}(E_2) \\
&+ 2a_2 b_2 \sqrt{N(N-1)} R_{12}(E_2)) \quad (\text{C1c})
\end{aligned}$$

$$\begin{aligned}
t_{21} &= (a_1 a_2 N R_{11}(E_2) + b_1 b_2 (N-1) R_{22}(E_2) \\
&+ \sqrt{N(N-1)} (a_2 b_1 + a_1 b_2) R_{21}(E_2)) \quad (\text{C1d})
\end{aligned}$$

If we substitute in these expressions a_i , b_i and R for their explicit forms (24), (25), and (35a), (35c), (35b), we obtain the expressions for t_{ij} given in Sec.V in (36), (37), (38), (39).

Appendix D: Calculation of the triplet wavefunction

As we show in the main text, there are two possible initial states (20): $|\varphi_{1,k}\rangle$ and $|\varphi_{2,k}\rangle$. Accordingly, there are two wavefunctions (14):

$$\begin{aligned}
|\Psi_1\rangle &= |\varphi_{1,k}\rangle + \frac{1}{E_1 - H_{eff}} H_{QP} |\varphi_{1,k}\rangle \\
&+ \frac{1}{E_1 - H_{PP} + i\varepsilon} H_{PQ} \frac{1}{E_1 - H_{eff}} H_{QP} |\varphi_{1,k}\rangle \quad (\text{D1a})
\end{aligned}$$

where

$$\begin{aligned} |\Psi_2\rangle &= |\varphi_{2,k}\rangle + \frac{1}{E_2 - H_{eff}} H_{QP} |\varphi_{2,k}\rangle \\ &+ \frac{1}{E_2 - H_{PP} + i\varepsilon} H_{PQ} \frac{1}{E_2 - H_{eff}} H_{QP} |\varphi_{2,k}\rangle \end{aligned} \quad (\text{D1b})$$

Next we use the properties of completeness of P and Q ($P + Q = 1$) and their orthogonality ($PQ = QP = 0$) to obtain from (D1a) and (D1b)

$$\begin{aligned} |\Psi_1\rangle &= |\varphi_{1,k}\rangle + \sum_{n,m=1}^2 |n\rangle \langle n| \frac{1}{E_1 - H_{eff}} |m\rangle \langle m| H_{QP} |\varphi_{1,k}\rangle \\ &+ \sum_{\substack{i,j=1 \\ k,k'}}^2 \left\{ |\varphi_{i,k}\rangle \langle \varphi_{i,k}| \frac{1}{E_1 - H_{PP} + i\varepsilon} |\varphi_{i,k'}\rangle \right. \\ &\times \left. \langle \varphi_{j,k'}| H_{PQ} |n\rangle \langle n| \frac{1}{E_1 - H_{eff}} |m\rangle \langle m| H_{QP} |\varphi_{1,k}\rangle \right\} \end{aligned} \quad (\text{D2})$$

$$\begin{aligned} |\Psi_2\rangle &= |\varphi_{2,k}\rangle + \sum_{n,m=1}^2 |n\rangle \langle n| \frac{1}{E_2 - H_{eff}} |m\rangle \langle m| H_{QP} |\varphi_{2,k}\rangle \\ &+ \sum_{\substack{i,j=1 \\ k,k'}}^2 \left\{ |\varphi_{i,k}\rangle \langle \varphi_{i,k}| \frac{1}{E_2 - H_{PP} + i\varepsilon} |\varphi_{i,k'}\rangle \right. \\ &\times \left. \langle \varphi_{j,k'}| H_{PQ} |n\rangle \langle n| \frac{1}{E_2 - H_{eff}} |m\rangle \langle m| H_{QP} |\varphi_{2,k}\rangle \right\} \end{aligned} \quad (\text{D3})$$

From these equations it follows immediately the expressions (40) and (41), which we write here in the following form:

$$\begin{aligned} |\Psi_1\rangle &= |\varphi_{1,k}\rangle + \sum_{m,n} |n\rangle R_{nm}(E_1) \langle m| H_{QP} |\varphi_{1,k}\rangle \\ &+ \xi^2 \sum_{q,i} \frac{|\varphi_{i,q}\rangle t_{i1}}{E_1(k) - E_i(q) + i\varepsilon} \end{aligned} \quad (\text{D4})$$

$$\begin{aligned} |\Psi_2\rangle &= |\varphi_{2,k}\rangle + \sum_{m,n} |n\rangle R_{nm}(E_2) \langle m| H_{QP} |\varphi_{2,k}\rangle \\ &+ \xi^2 \sum_{q,i} \frac{|\varphi_{i,q}\rangle t_{i2}}{E_2(k) - E_i(q) + i\varepsilon} \end{aligned} \quad (\text{D5})$$

In order to obtain photon wavefunction in a configuration space we multiply (D4) and (D5) from the left by bra vector $\langle x|$, and taking into account that $\langle x|n\rangle = 0$, $\langle x|\varphi_{i,k}\rangle = e^{ikx}|\varphi_i\rangle$, we obtain:

$$\langle x|\Psi_1\rangle = e^{ikx} |\varphi_{1,k}\rangle + \xi^2 \sum_{i=1}^2 J_{i,1} t_{i1} |\varphi_i\rangle \quad (\text{D6})$$

$$\langle x|\Psi_2\rangle = e^{ikx} |\varphi_{2,k}\rangle + \xi^2 \sum_{i=1}^2 J_{i,2} t_{i2} |\varphi_i\rangle \quad (\text{D7})$$

$$J_{i,j} = \sum_q \frac{e^{iqx}}{E_j(k) - E_i(q) + i\varepsilon} \quad (\text{D8})$$

Below we calculate the quantities $J_{i,j}$. The result is as follows:

$$J_{11} = J_{22} = -i \frac{L}{v_g} e^{ik|x|} \quad (\text{D9})$$

$$J_{12} = -i \frac{L}{v_g} e^{i(k - \frac{\Omega_R}{v_g})|x|} \quad (\text{D10})$$

$$J_{21} = -i \frac{L}{v_g} e^{i(k + \frac{\Omega_R}{v_g})|x|} \quad (\text{D11})$$

With the account of these results we obtain for the photon wavefunctions (D6), (D7) the expressions (42) and 43) from the main text.

Appendix E: Calculation of $J_{i,j}$

From (29), (30) we find the energy difference in the denominator of (D8):

$$\begin{aligned} E_i(k) - E_i(q) &= \omega_k - \omega_q = v_g(k - q); \\ E_1(k) - E_2(q) &= \omega_k - \omega_q + \Omega_R = v_g(k - q + \frac{\Omega_R}{v_g}); \\ E_2(k) - E_1(q) &= \omega_k - \omega_q - \Omega_R = v_g(k - q - \frac{\Omega_R}{v_g}) \end{aligned} \quad (\text{E1})$$

As an example we calculate below the quantity J_{12} (D10) where we substitute the summation over q for the integration:

$$J_{12} = \frac{L}{2\pi} \int_{-\infty}^{+\infty} \frac{e^{iqx}}{\omega_k - \omega_q - \Omega_R + i\varepsilon} dq \quad (\text{E2})$$

The main contribution to this integral comes from the region where $\omega_q \approx \omega_k - \Omega_R$. Since ω_q is the even function of q , it can be approximated away from the cutoff frequency as $\omega_q \equiv v_g|q|$. In this case the poles of the integrand (E2) in the q plane are located near the points $q \approx \pm q_0$ where $q_0 = (k - \Omega_R/v_g)$. From denominator in (E2) we see that one pole is located in the upper half of the q plane, $q = q_0 + i\varepsilon$, the other pole is located in the lower half of the q plane, $q = -q_0 - i\varepsilon$. For positive x , when calculating the integral (E2) we must close the path in the upper plane. For negative x the path should be closed in lower plane. Thus, we obtain:

$$J_{12} = -i \frac{L}{\hbar v_g} e^{i(k - \frac{\Omega_R}{v_g})|x|} \quad (\text{E3})$$

The quantities J_{11} , J_{22} (D9) and J_{21} (D11) can be calculated by the same procedure.

* Electronic address: yakovgreenberg@yahoo.com

¹ J. Q. You and F. Nori, Atomic Physics and Quantum Optics Using Superconducting Circuits, *Nature*, Vol. **474**, No. 7353, 589 (2011).

² S. M. Girvin, M. H. Devoret and R. J. Schoelkopf, Circuit QED and Engineering Charge-based Superconducting Qubits, *Physica Scripta* **T137**, 014012 (2009).

³ Y. A. Pashkin, O. Astafiev, T. Yamamoto, Y. Nakamura and J. S. Tsai, Josephson Charge Qubits: a Brief Review, *Quantum Information Processing* **8**, 55 (2009).

⁴ B. C. Sanders, Quantum Optics in Superconducting Circuits, *AIP Conference Proceedings* **1398**, 46 (2011).

⁵ T. Niemczyk, F. Deppe, H. Huebl, E. P. Menzel, F. Hocke, M. J. Schwarz, J. J. Garcia-Ripoll, D. Zueco, T. Hmmer, E. Solano, A. Marx and R. Gros Circuit Quantum Electrodynamics in the Ultrastrong-coupling Regime, *Nature Physics* **6**, 772 (2010).

⁶ S. , J. Twamley and G. J. Milburn, Giant Kerr Nonlinearities in Circuit Quantum Electrodynamics, *Phys. Rev. Lett.* **103**, 150503 (2009).

⁷ A. A. Abdumalikov, Jr., O. Astafiev, A. M. Zagorskin, Yu. A. Pashkin, Y. Nakamura and J. S. Tsai, Electromagnetically Induced Transparency on a Single Artificial Atom, *Phys. Rev. Lett.* **104**, 193601 (2010).

⁸ J. Joo, J. Bourassa, A. Blais and B. C. Sanders, Electromagnetically Induced Transparency with Amplification in Superconducting Circuits, *Phys. Rev. Lett.* **105**, 073601 (2010).

⁹ Hai-Chao Li and Guo-Qin Ge Electromagnetically Induced Transparency using a Artificial Molecule in Circuit Quantum Electrodynamics Optics, *Photonics Journal* **3**, 29 (2013).

¹⁰ M. Baur, S. Filipp, R. Bianchetti, J. M. Fink, M. Goppl, L. Steffen, P. J. Leek, A. Blais, and A. Wallraff Measurement of Autler-Townes and Mollow Transitions in a Strongly Driven Superconducting Qubit, *Phys. Rev. Lett.* **102**, 243602 (2009).

¹¹ O. Astafiev, A. M. Zagorskin, A. A. Abdumalikov Jr., Yu. A. Pashkin, T. Yamamoto, K. Inomata, Y. Nakamura, J. S. Tsai., Resonance Fluorescence of a Single Artificial Atom, *Science*, **327**, 840 (2010).

¹² Io-Chun Hoi, T. Palomaki, J. Lindkvist, G. Johansson, P. Delsing, and C. M. Wilson Generation of Nonclassical Microwave States Using an Artificial Atom in 1D Open Space, *Phys. Rev. Lett.* **108**, 263601 (2012)

¹³ C. Lang, D. Bozyigit, C. Eichler, L. Steffen, J. M. Fink, A. A. Abdumalikov, Jr., M. Baur, S. Filipp, M. P. da Silva, A. Blais, and A. Wallraff Observation of Resonant Photon Blockade at Microwave Frequencies, *Phys. Rev. Lett.* **106** 243601 (2011)

¹⁴ D. M. Toyli, A. W. Eddins, S. Boutin, S. Puri, D. Hover, V. Bolkhovsky, W. D. Oliver, A. Blais, and I. Siddiqi Resonance fluorescence from an artificial atom in squeezed vacuum, arXiv: 1602.03240v1

¹⁵ M. A. Sillanpaa, J. Li, K. Cicak, F. Altomare, J. I. Park, R. W. Simmonds, G. S. Paraoanu, and P. J. Hakonen., Autler-Townes Effect in a Superconducting Three-Level System, *Phys. Rev. Lett.* **103**, 193601 (2009).

¹⁶ 14. Mollow, B. R. Power spectrum of light scattered by two-level systems. *Phys. Rev.* **188**, 1969 (1969).

¹⁷ N. Auerbach and V. Zelevinsky Super-radiant dynamics, doorways, and resonances in nuclei and other open mesoscopic systems, *Rep. Progr. Phys.* **74**, 106301 (2011).

¹⁸ G. L. Celardo, A. M. Smith, S. Sorathia, V. G. Zelevinsky, R. A. Sen'kov, and L. Kaplan, Transport through nanostructures with asymmetric coupling to the leads, *Phys. Rev. B* **82**, 165437 (2010).

¹⁹ Ya. S. Greenberg, N. Merrigan, A. Tayebi, and V. Zelevinsky Quantum signal transmission through a single-qubit chain, *Eur. Phys. J.* **86**, 368 (2013).

²⁰ Ya. S. Greenberg and A. A. Shtygashev Non-Hermitian Hamiltonian approach to the microwave transmission through one-dimensional qubit chain, *Phys. Rev. A* **92**, 063835 (2015).

²¹ I. Rotter Dynamics of quantum systems, *Phys. Rev E* **64** 036213(2001).